ISSN: 2834-7706

Research Article

Journal of Mathematical Techniques and Computational Mathematics

Dynamical and Atmospheric Evolution of TOI-5734 b: a Hot Sub-Neptune at The Edge of The Radius Valley

Bijay Kumar Sharma*

Electronics and Communication Engineering Department, National Institute of Technology, Patna 800005, India

*Corresponding Author
Bijay Kumar Sharma, Electronics and Communication Engineering Department,National Institute of Technology, Patna 800005, India.

Submitted: 2026, Mar 23; **Accepted**: 2026, Apr 15; **Published**: 2026, Apr 23

Citation: Sharma, B. K. (2026). Dynamical and Atmospheric Evolution of TOI-5734 b: a Hot Sub-Neptune at The Edge of The Radius Valley. *J Math Techniques Comput Math, 5*(4), 01-12

Abstract

We present a dynamical and structural investigation of the recently discovered hot sub-Neptune TOI-5734 b, a short-period exoplanet located near the upper boundary of the radius valley. Identified through photometric observations by the Transiting Exoplanet Survey Satellite and radial-velocity measurements from the HARPS-N spectrograph at the Galileo National Telescope, the planet orbits a young K-dwarf star at a separation of approximately 0.06 AU with an orbital period of 6.18 days. With a radius of 2.1 $R_{\oplus}$ and mass of 9.1 $M_{\oplus}$, TOI 5734 b lies in the transitional regime between super-Earths and gas-rich sub-Neptunes. Its bulk density indicates a predominantly rocky interior with a residual volatile envelope. The intense stellar irradiation corresponding to an equilibrium temperature of 688 K strongly favors ongoing atmospheric escape. Evolutionary considerations suggest that the planet may lose most of its primordial atmosphere within 3×10^8 years. We analyze the orbital and angular-momentum evolution of the system using a primary-centric dynamical framework, examining tidal dissipation, migration history, and long- term orbital stability. The planet's present position near the radius gap supports atmospheric erosion driven by photoevaporation and/or core-powered mass loss. TOI-5734 b thus provides an important laboratory for understanding the physical mechanisms that sculpt the dominant intermediate-mass planet population and offers key insights into the evolutionary pathways linking sub-Neptunes and super-Earths.

Keywords: Planet, Star Interactions, Exoplanets, Stellar Evolution, Orbital Dynamics

1. Introduction

The discovery of exoplanets over the past three decades has revealed a remarkable diversity of planetary systems, fundamentally reshaping our understanding of planet formation and evolution. Space-based transit missions such as the Transiting Exoplanet Survey Satellite and precision radial-velocity instruments including the HARPS-N spectrograph have enabled the detection and characterization of thousands of planets spanning a wide range of masses, sizes, and orbital architectures [1,2]. Among these populations, planets with radii between that of Earth and Neptune — commonly termed super-Earths and sub-Neptunes — constitute the most abundant class of exoplanets in the Galaxy. Statistical surveys reveal a bimodal distribution of small-planet radii with a deficit near 1.5–2.0 *R* , commonly termed the radius valley [3].

This feature, known as the *radius valley or radius gap,* separates two dominant planetary populations: smaller, high-density rocky planets and larger, low-density planets possessing significant volatile envelopes [3,4]. The radius valley is widely interpreted as a consequence of atmospheric es- cape driven by photoevaporation or core-powered mass loss [5,6]. The physical origin of the ra- dius valley is a major topic in modern exoplanetary science. One

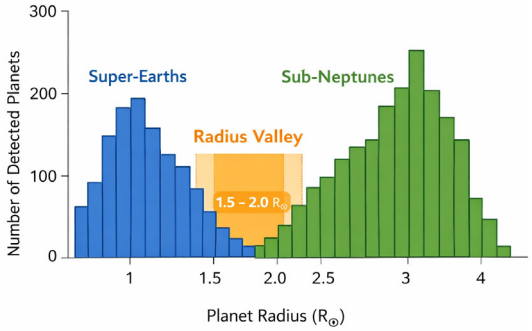

Figure 1: Bimodal distribution of exoplanet radii showing the radius valley between super-Earths and sub-Neptunes.

Leading explanation attributes the gap to photoevaporation, in which intense stellar X-ray and extreme-ultraviolet radiation heats planetary atmospheres and drives hydrodynamic escape,

preferentially stripping gaseous envelopes from low-mass planets [6,7]. Figure 1 shows the bimodal distribution of planetary radii. An alternative mechanism, known as core-powered mass loss, proposes that the thermal luminosity of a planet's cooling interior can erode primordial atmospheres even in the absence of strong stellar irradiation [6]. Core-powered mass loss is an atmospheric escape process driven by the release of thermal energy stored in a planet's interior. As the planetary core cools, the resulting heat flux inflates the gaseous envelope and can drive hydrodynamic escape, particularly for low-gravity planets with thin primordial atmospheres. Both processes predict that planets near the radius valley represent transitional evolutionary states linking gas-rich sub-Neptunes and rocky super-Earths.

Transitional planets located near the edges of the radius valley are therefore valuable laboratories for studying atmospheric erosion, interior structure, and long-term planetary evolution. Their present properties encode information about formation pathways, migration history, and star–planet interactions. In particular, short-period sub-Neptunes orbiting close to their host stars experience intense irradiation and strong tidal forces, accelerating atmospheric escape and orbital evolution [8,9].

In this context, the recently discovered hot sub-Neptune TOI-5734 b provides an important new case study. Identified using transit observations from TESS and radial-velocity follow-up from HARPS-N, the planet orbits a young K-dwarf star on a compact 6.18-day orbit. With a radius of 2.1 R and mass of 9.1 M , TOI-5734 b lies near the upper boundary of the radius valley, placing it in the transitional regime between super-Earths and gas-rich sub-Neptunes [10]. Its close orbital separation (a 0.06 AU) results in strong stellar irradiation and elevated equilibrium temperatures, conditions favorable for ongoing atmospheric escape.

The location of TOI-5734 b near the radius valley suggests that it may be undergoing significant structural and atmospheric transformation. Its bulk density implies a predominantly rocky interior with a residual volatile envelope, consistent with advanced atmospheric stripping. Moreover, theoretical studies indicate that such planets may lose their primordial atmospheres on timescales of a few hundred million years, eventually evolving into dense, atmosphere-poor super-Earths.

In this work, we investigate the structural, atmospheric, and dynamical evolution of TOI-5734 b. We analyze its physical properties in the context of radius-valley populations, examine mechanisms of atmospheric escape, and explore orbital evolution driven by tidal interactions. Transitional systems such as TOI-5734 b offer critical insight into the processes that shape the dominant intermediate-mass planet population and help bridge observational gaps between formation theory and present-day planetary demographics.

2. Observational Properties Of The Toi-5734 System

2.1 Host Star Properties

TOI-5734 is a relatively young K-type dwarf star located at a distance of approximately 106 light-years. Stellar classification places it between spectral types K3 and K4, indicating a moderately cool photosphere compared to the Sun. The star has a mass of approximately 0.72 M and a radius of 0.64 R , making it smaller and less luminous than solar-type stars. Its effective temperature is estimated to be Teff 4750 K, consistent with late K-dwarf stellar atmospheres. The relatively young age of the system suggests enhanced stellar activity and strong high-energy radiation environments, both of which are critical factors in planetary atmospheric evolution. Young K-dwarfs are known to exhibit elevated levels of X-ray and extreme- ultraviolet emission, which can significantly influence atmospheric escape processes on close-in planets.

2.2 Planetary Parameters of TOI-5734 b

TOI-5734 b is a short-period exoplanet discovered using transit photometry from the Transiting Exoplanet Survey Satellite and con- firmed via radial-velocity measurements from the HARPS-N spectrograph [1,2 10]. The planet orbits its host star with a period of 6.18 days at a semi major axis of approximately 0.06 AU.

With a measured radius of 2.1 R and mass of 9.1 M , TOI-5734b falls into the transitional regime between super-Earths and sub-Neptunes. Its bulk density is lower than that of Earth, suggesting the presence of a volatile-rich envelope surrounding a predominantly rocky core.

The close orbital separation exposes the planet to intense stellar irradiation. Assuming radiative equilibrium and efficient heat redistribution, the planetary equilibrium temperature is estimated to be $T_{eq} \approx 688$ K. Such conditions favor atmospheric escape and long-term structural evolution.

2.3 Orbital Configuration

The compact orbit of TOI-5734 b places it well inside the inner regions of the planetary system, where tidal forces and star–planet interactions are strong. Except at the Clarke orbits, tidal torques operate on planetary orbits, causing energy dissipation and angular- momentum exchange. These effects intensify strongly at small orbital separations [9]. The system therefore provides a natural laboratory for studying coupled orbital and atmospheric evolution.

The present orbital configuration also suggests a possible migration history. Planets of comparable mass are believed to form beyond the snow line and subsequently migrate inward through disk-driven processes or tidal evolution. In the sub synchronous tidal regime ($\Omega > \omega_{\star}$), the orbital motion exceeds the stellar spin rate, causing the tidal bulge raised on the star to lag behind the planet. The resulting tidal torque transfers orbital angular momentum to the stellar spin and internal dissipation, leading to stellar spin-up and progressive orbital decay. This configuration drives continued inward migration along a collapsing tidal branch, often referred to as a tidal "death spiral." The current position of TOI-5734 b near the radius valley may thus reflect a combined history of migration, irradiation, and atmospheric erosion.

3. Radius Valley Context And Population Statistics

3.1 Bimodal Radius Distribution

Large-scale statistical surveys of transiting exoplanets have revealed that the distribution of planetary radii is not continuous but exhibits a clear bimodal structure as shown in Figure 1 Two dominant populations emerge: compact, high-density rocky planets with radii below 1.5 R , and larger, low-density planets with substantial volatile envelopes above $\sim 2.0\ R_{\oplus}$ [3,4].

Between these populations lies a deficit of planets spanning radii $\sim 1.5–2.0\ R_{\oplus}$, commonly referred to as the *radius valley or radius gap.* This feature is now considered one of the most significant observational signatures in exoplanet demographics. The bimodal distribution is illustrated in Figure 1.

3.2 Physical Interpretation of the Radius Valley

The radius valley is widely interpreted as an evolutionary boundary separating planets that have retained thick gaseous envelopes from those that have lost their primordial atmospheres. Because planetary radius is strongly influenced by atmospheric mass fraction, even modest envelope loss can shift a planet from the sub-Neptune regime into the super-Earth regime.

Two principal mechanisms have been proposed to explain this phenomenon.

3.2.1 Photoevaporation-Driven Atmospheric Loss

In this scenario, high-energy stellar radiation in the X-ray and extreme ultraviolet bands heats the upper planetary atmosphere, driving hydrodynamic outflows that remove volatile gases over time [6,7]. Low-mass planets in close-in orbits are particularly vulnerable to this process, as their gravitational binding energy is insufficient to retain light gases under intense irradiation.

3.2.2 Core-Powered Mass Loss

An alternative mechanism proposes that atmospheric escape can be powered by the planet's internal thermal luminosity. As the planetary core cools after formation, its residual heat can drive atmospheric escape even in the absence of strong stellar irradiation [6]. This process is particularly effective for intermediate-mass planets with thin primordial envelopes.

Both mechanisms predict that planets near the radius valley represent transitional evolutionary states and that the valley itself traces a boundary in atmospheric retention efficiency.

3.3 Transitional Planets as Evolutionary Probes

Planets located near the edges of the radius valley provide critical insight into the physical processes governing planetary evolution. Their present properties reflect the combined effects of formation history, atmospheric erosion, and orbital dynamics.

TOI-5734 b lies near the upper boundary of the radius valley with a radius of 2.1 R , placing it at the transition between rocky super-Earths and gas-rich sub-Neptunes. Its position suggests that it may be undergoing significant atmospheric stripping, potentially evolving toward a denser, atmosphere-poor state.

The system therefore offers an opportunity to investigate how irradiation, tidal interactions, and internal planetary structure interact to sculpt the dominant intermediate-mass planet population.

4 Interior Structure and Bulk Composition

4.1 Mean Density and Structural Inference

Figure 2 shows the location of TOI-5734 b in the mass–radius plane relative to comparison planets and theoretical composition models.

The bulk composition of TOI-5734 b is inferred from its position in the mass–radius plane (Figure 2). As shown in Figure 2, the planet lies in the transitional regime between rocky super-Earths and volatile-rich sub-Neptunes. The measured mass and radius of TOI-5734 b allow estimation of its bulk density,

$$\rho_p = \frac{3M_p}{4\pi R_p^3}. \tag{1}$$

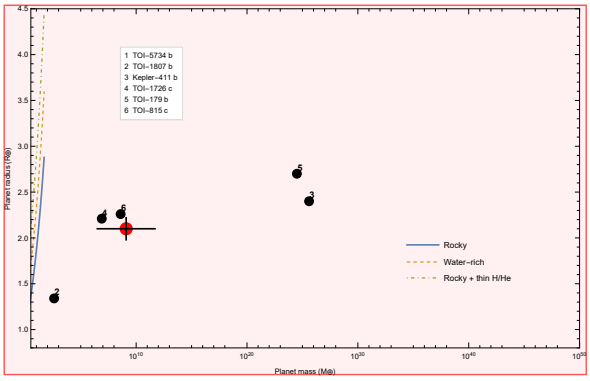

Figure 2: Mass–radius diagram showing the position of TOI-5734 b (red point with error bars; Point 1) relative to comparison planets (numbered black points, 2–6). Curves show representative internal composition models.

With $Mp = 9.1\ M_{\oplus}$ and $Rp = 2.1\ R_{\oplus}$, the inferred density is lower than that of Earth, indicating that the planet is unlikely to be composed solely of iron and silicate rock. Instead, the density suggests the presence of a volatile-rich envelope surrounding a dense interior core.

4.2 Possible Internal Structure

Planets in the mass–radius regime of TOI-5734 b are typically modeled as multi-layered bodies consisting of:

- A dense rocky or iron-rich core,
- A silicate mantle,
- A volatile envelope composed of H/He and/or water-rich layers.

Even a small atmospheric mass fraction can significantly inflate

the planetary radius. Structural models therefore permit several possible configurations:
(i) A rocky super-Earth core with a thin H/He envelope,
(ii) A water-rich world with high-pressure ice layers,
(iii) A remnant sub-Neptune that has lost much of its primordial atmosphere.

4.3 Location in the Radius Valley Regime

The radius of TOI-5734 b (2.1 R) places it near the upper boundary of the radius valley, where planets transition from gas-rich sub-Neptunes to predominantly rocky super-Earths. This suggests that the planet may represent an intermediate evolutionary stage in which atmospheric mass loss is actively reshaping its structure.

5 Atmospheric Escape And Thermal Evolution

Figure 3 illustrates the expected atmospheric mass evolution under irradiation-driven escape. The temporal evolution of the envelope mass fraction is modeled using a power-law decay of the form:

$$f_{\mathrm{env}}(t) = f_0 \left(\frac{t}{t_0}\right)^{-\alpha}, \tag{2}$$

where f_{env} is the envelope mass fraction at time t, f_0 is the initial envelope fraction at reference time t_0, and α is the atmospheric loss exponent determined by the escape efficiency and irradiation environment. The resulting evolutionary track is shown in Figure 3.

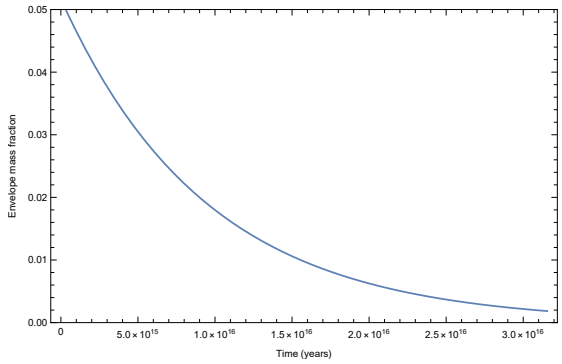

Figure 3: Illustrative atmospheric mass-loss evolution of TOI-5734 b un- der stellar irradiation. The declining envelope fraction indicates progressive stripping of the primordial volatile layer, consistent with migration toward the radius-valley boundary.

The declining envelope fraction indicates progressive stripping of the primordial volatile layer, consistent with evolutionary migration toward the radius-valley boundary. Atmospheric escape from close-in sub-Neptunes is generally driven by stellar X-ray and extreme-ultraviolet (XUV) irradiation, which heats the upper atmosphere and can power hydrodynamic outflows [7,11]. In the energy-limited regime, the mass-loss rate is approximated by

$$\dot{M} = \frac{\eta \pi R_p^3 F_{\mathrm{XUV}}}{G M_p K}, \tag{3}$$

where η is the heating efficiency, Rp and Mp are the planetary radiusand mass, FXUV is the incident stellar high-energy flux, and K accounts for Roche-lobe effects [12]. Detailed evolutionary calculations require numerical integration of this loss rate coupled with thermal-structure models. For the illustrative evolutionary track shown in Figure 3, we adopt a parametrized exponential decay of the envelope mass fraction models based on the energy-limited formalism indicate that TOI-5734 b may lose most of its primordial atmosphere on a timescale of 3 10^8 yr for plausible heating efficiencies [7,11,12].

$$f_{\mathrm{env}}(t) = f_0 \exp\left[-\frac{(t - t_0)}{\tau}\right], \tag{4}$$

where $f_{\mathrm{env}}(t)$ is the envelope mass fraction at time t, f_0 is the initial envelope fraction at reference epoch t_0, and τ is a characteristic atmospheric-loss timescale. We adopt illustrative parameters f_0 = 0.05, t_0 = 10^7 yr, and τ = 3 × 10^8 yr, consistent with escape timescales estimated for strongly irradiated sub-Neptunes.

5.1 Stellar Irradiation Environment

TOI-5734 b orbits its host star at a separation of approximately 0.06 AU, subjecting it to intense stellar irradiation. Assuming radiative equilibrium, its equilibrium temperature is estimated as

$$T_{\mathrm{eq}} \approx 688 \text{ K}, \tag{5}$$

placing the planet in the hot sub-Neptune regime.

Young K-dwarf stars are known to emit elevated levels of X-ray and extreme-ultraviolet radiation, which can strongly heat the upper planetary atmosphere and drive mass loss.

5.2 Atmospheric Loss Timescale

This simplified parametrization captures the gradual erosion of the volatile envelope under sustained stellar irradiation while remaining consistent with energy-limited escape theory. Evolutionary escape models based on the energy-limited formalism (Watson et al. 1981; Lammer et al. 2003; Erkaev et al. 2007) indicate that TOI-5734 b may lose most of its primordial atmosphere on a timescale of ~ 3×10^8 yr for plausible heating efficiencies.

$$\tau_{\mathrm{atm}} \sim 3 \times 10^8 \text{ yr}. \tag{6}$$

Such rapid atmospheric erosion would drive the planet toward a denser, atmosphere-poor configuration, consistent with migration across the radius valley.

5.3 Evolutionary Implications

Atmospheric escape modifies planetary radius, density, and composition over time. TOI-5734 b therefore provides a direct probe of evolutionary pathways linking sub-Neptunes and super-Earths.

6 ORBITAL EVOLUTION IN THE PRIMARY-CENTRIC FRAMEWORK

6.1 System Parameters Used in the Dynamical Analysis

Table 1 lists the stellar and planetary parameters adopted for the present orbital and tidal evolution analysis.

6.2 Two synchronous (Clarke) orbits in the primary-centric formalism

For a two-body star–planet system in a circular orbit, the total angular momentum may be written as

$$J_T = C_\star \omega_\star + L_{\rm orb}, \tag{7}$$

where

$$L_{\rm orb} = \mu\sqrt{G(M_\star + M_p)a}, \tag{8}$$

$$\mu = \frac{M_\star M_p}{M_\star + M_p}, \tag{9}$$

and

$$C_\star = k_\star M_\star R_\star^2 \tag{10}$$

is the moment of inertia of the host star. The orbital angular velocity is

$$\Omega = \sqrt{\frac{G(M_\star + M_p)}{a^3}}. \tag{11}$$

Solving the total angular momentum equation for the stellar spin gives

$$\omega_\star = \frac{J_T - \mu\sqrt{G(M_\star + M_p)a}}{C_\star}. \tag{12}$$

Hence the ratio of stellar spin to orbital angular velocity becomes

$$\frac{\omega_\star}{\Omega} = \frac{J_T}{C_\star\sqrt{G(M_\star + M_p)}}\, a^{3/2} - \frac{\mu}{C_\star}\, a^2. \tag{13}$$

Defining

$$A = \frac{J_T}{C_\star\sqrt{G(M_\star + M_p)}}, \qquad F = \frac{\mu}{C_\star}, \tag{14}$$

Parameter	Symbol	Value	Reference
Planetary Parameters			
Planet mass	M_p	9.1 $M_\oplus$	(Filomeno et al. 2026)
Planet radius	R_p	2.1 $R_\oplus$	(Filomeno et al. 2026)
Orbital period	$P_{\rm orb}$	6.18 d	(Filomeno et al. 2026)
Semi-major axis	$a_{\rm now}$	0.059 AU	(Filomeno et al. 2026)
Equilibrium temperature	$T_{\rm eq}$	~ 688 K	(Filomeno et al. 2026)
Bulk density	ρ_p	—	Derived in this work
Stellar Parameters			
Stellar mass	$M_\star$	0.72 $M_\odot$	(Filomeno et al. 2026)
Stellar radius	$R_\star$	0.64 $R_\odot$	(Filomeno et al. 2026)
Effective temperature	$T_{\rm eff}$	4750 K	(Filomeno et al. 2026)
Stellar age	—	few Gyr	(Filomeno et al. 2026)
Spectral type	—	K3–K4 V	(Filomeno et al. 2026)
Derived Dynamical Parameters			
Roche-limit distance	$a_{\rm Roche}$	0.0053 AU	This work
Inner Clarke orbit	a_{G1}	—	This work
Outer Clarke orbit	a_{G2}	—	This work
Tidal decay timescale	$\tau_{\rm tidal}$	~ 10^9 yr	This work
Atmospheric loss timescale	$\tau_{\rm atm}$	~ 3×10^8 yr	This work

Table 1: Adopted System Parameters of the TOI-5734 Planetary System.

we obtain the compact primary-centric relation

$$\frac{\omega_\star}{\Omega} = Aa^{3/2} - Fa^2. \tag{15}$$

For notational consistency with the primary-centric formalism adopted in this work, the coefficient previously denoted by E is redefined as A. The constants are defined as

$$A = \frac{J_T}{C_\star\sqrt{G(M_\star + M_p)}}, \qquad F = \frac{\mu}{C_\star}, \tag{16}$$

where J_T is the total angular momentum of the system, $C_\star$ is the stellar moment of inertia, and μ is the reduced mass. The synchronous orbits, also referred to here as the Clarke orbits, are

obtained from the condition

$$\omega_\star = \Omega, \tag{17}$$

that is,

$$Aa^{3/2} - Fa^2 = 1. \tag{18}$$

Letting $x = \sqrt{a}$, Eq. (18) becomes

$$-Ax^3 + Fx^4 + 1 = 0. \tag{19}$$

This quartic admits, in general, two physically relevant positive roots, corresponding to two synchronous radii:

$$a_{G1} = x_1^2, \qquad a_{G2} = x_2^2, \qquad (a_{G1} < a_{G2}). \tag{20}$$

Figure 4 illustrates the inner synchronous condition defining the inner Clarke orbit. The inner synchronous condition in the primarycentric framework is illustrated in Figure 4. The inner root a_{G1} is the inner Clarke orbit and represents the unstable synchronous boundary, while the outer root a_{G2} is the outer Clarke orbit associated with the stable tidal equilibrium branch shown in Figure 8.

6.3 Stability of the Clarke orbits

The dynamical nature of the two Clarke orbits follows from total energy considerations. For a tidally interacting star–planet system

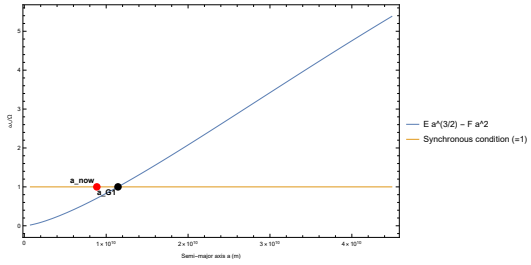

Figure 4. Primary-centric synchronization condition. The inner Clarke orbit (a_{G1}) is defined by the intersection with the synchronous state, while the present orbit (a_{now}) lies interior to a_{G1}, indicating inward tidal evolution along the collapsing branch. The outer Clarke orbit lies beyond the plotted range. Credit: Original figure created by the author.

with fixed total angular momentum, equilibrium configurations occur at stationary points of the total mechanical energy,

$$E_{\mathrm{tot}} = E_{\mathrm{orb}} + E_{\mathrm{rot}}, \tag{21}$$

where E_{orb} and E_{rot} denote the orbital and rotational energies, respectively.

Equilibrium requires

$$\frac{dE_{\mathrm{tot}}}{da} = 0,$$

which yields the synchronization condition defining the Clarke orbits. The nature of the equilibrium depends on the curvature of the energy profile. The inner Clarke orbit a_{G1} corresponds to a local maximum of the total energy and therefore represents an unstable equilibrium configuration: small perturbations drive the system away from this state. In contrast, the outer Clarke orbit a_{G2} occurs at a local minimum of the total energy and constitutes a stable equilibrium configuration toward which nearby states evolve.

The variation of the total mechanical energy with orbital separation.

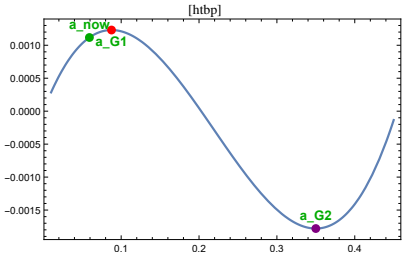

Figure 5: Total mechanical energy as a function of orbital separation for TOI-5734 b in the primary-centric framework. The inner Clarke orbit (a_{G1}) corresponds to a local maximum of the total energy and is therefore an unstable equilibrium point, whereas the outer Clarke orbit (a_{G2}) corresponds to a local minimum and represents a stable equilibrium configuration. The present orbit (a_{now}) lies to the left of a_{G1}, indicating that the planet is trapped on the collapsing tidal branch and is undergoing inward orbital evolution.

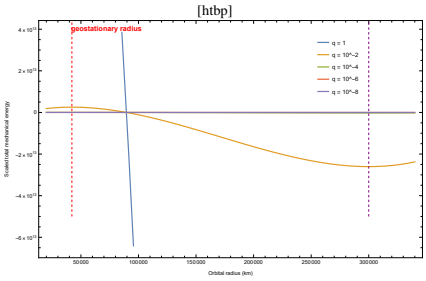

Figure 6: Illustrative dependence of the total-energy profile on the mass ratio $q = m/M$. For large q, the total mechanical energy has a pronounced N-shaped form, with the inner Clarke orbit corresponding to an unstable maximum and the outer Clarke orbit to a stable minimum. As $q \to 0$, the energy relief progressively flattens, and the unstable peak near the inner synchronous orbit becomes increasingly shallow. In the ideal two-body limit, this approaches the nearly neutral behavior associated with the geostationary configuration of artificial satellites. **Credit:** Original figure created by the author.

is shown in Figure 5. The present orbit lies interior to a_{G1}, indicating that TOI-5734 b is trapped on the collapsing tidal branch and is undergoing inward orbital evolution.

As shown in Figure 6, the total-energy peak near the inner Clarke orbit becomes progressively flatter as the mass ratio q decreases. Figure 7 illustrates the dependence of the Clarke-orbit topology on the mass ratio $q = m/M$. In the limit of an infinitesimal secondary ($q \to 0$), the total-energy barrier near the inner Clarke orbit becomes extremely shallow. In this regime the inner synchronous orbit $aG1$ remains physically accessible (tangible), while the outer equilibrium a_{G2} effectively recedes to very large separations and becomes dynamically irrelevant. This limiting behavior corresponds to the artificial-satellite case, where the geostationary orbit represents the practical synchronous configuration. As the mass ratio increases ($q \gtrsim 0.2$), the energy topology changes: the outer Clarke

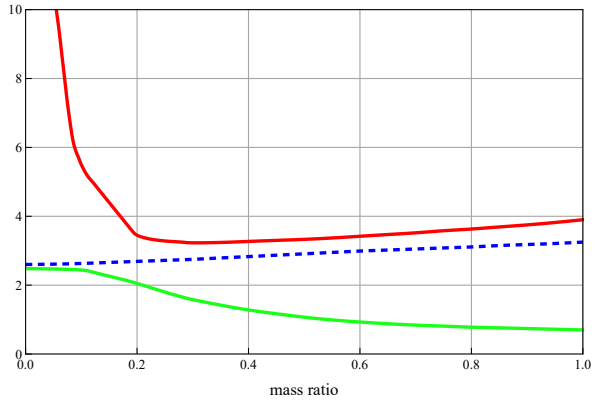

Figure 7: Refined reconstructed version of Figure 1 from (Sharma 2025), showing the variation of the three characteristic curves with the mass ratio q. The inner Clarke orbit a_{G1} is represented by the green curve, the outer Clarke orbit a_{G2} by the red curve, and the synchronous orbit a_{syn} by the blue dotted curve. **Credit:** Reconstructed by the author using Mathematica [13].

orbit a_{G2} becomes the dynamically meaningful equilibrium configuration, while the inner Clarke orbit a_{G1} loses its physical relevance. This transition arises because increasing q enhances the contribution of orbital angular momentum relative to the stellar rotational reservoir, thereby shifting the global minimum of the total mechanical energy toward the outer synchronous orbit. In the comparable-mass regime ($0.2 \lesssim q \leq 1$), therefore, the system evolves toward the outer stable equilibrium at a_{G2}, whereas the inner equilibrium becomes effectively intangible.

Figure 6 shows how the topology of the Clarke orbits depends on the mass ratio $q = m/M$. In the limit $q \to 0$, the total-energy barrier near the inner Clarke orbit becomes extremely shallow, so that the inner synchronous orbit a_{G1} remains physically accessible (tangible), while the outer equilibrium a_{G2} effectively recedes to very large separations and becomes dynamically irrelevant. This corresponds to the artificial-satellite limit, where the geostationary orbit represents the practical synchronous configuration. As the mass ratio increases ($q \gtrsim 0.2$), the topology changes: the outer Clarke orbit a_{G2} becomes the dynamically relevant equilibrium, whereas the inner Clarke orbit a_{G1} loses physical significance as shown in Figure 7. This shift occurs because increasing q enhances the orbital angular momentum relative to the stellar rotational reservoir, thereby moving the global minimum of the total mechanical energy toward the outer synchronous orbit. In the comparable-mass regime ($0.2 \lesssim q \leq 1$), the system therefore evolves toward the stable equilibrium at a_{G2}.

6.4 Present location of TOI-5734 b relative to the inner Clarke Orbit

For TOI-5734 b, the observed orbital period is

$$P_{\rm orb} \simeq 6.18 \text{ d}, \tag{22}$$

while the stellar rotation period is

$$P_{\rm rot} \simeq 11.1 \text{ d}. \tag{23}$$

Therefore,

$$P_{\rm orb} < P_{\rm rot}, \tag{24}$$

or equivalently,

$$\Omega > \omega_{\star}. \tag{25}$$

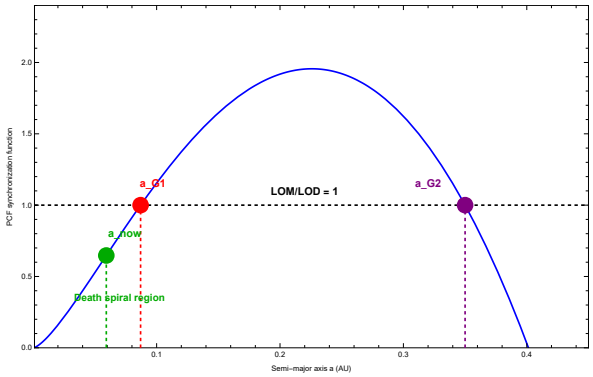

Figure 8: Variation of the angular-momentum ratio $\Lambda(a)$ = LOM/LOD with semi-major axis for TOI-5734 b. The present orbit $a_{\rm now}$ lies interior to the inner Clarke orbit $a_{G1,}$ indicating inward tidal evolution along the collapsing branch.

Using the synchronous condition in its corotation form,

$$\Omega = \omega_{\star} = \frac{2\pi}{P_{\rm rot}}, \tag{26}$$

the inner Clarke orbit is approximately

$$a_{G1} \approx \left[\frac{G(M_\star + M_p)}{\omega_\star^2}\right]^{1/3} \approx 0.087 \text{ AU}, \tag{27}$$

whereas the observed semi-major axis is

$$a_{\text{now}} \approx 0.0607 \text{ AU}. \tag{28}$$

Hence,

$$a_{\text{now}} < a_{G1}. \tag{29}$$

This inequality is the key dynamical result: TOI-5734 b lies interior to the inner Clarke orbit and is therefore not on the outward-migration branch. Instead, it is trapped in the inward-decaying tidal branch.

The angular-momentum evolution is illustrated in Figure 8. Bell-shaped synchronization curve in the Primary-Centric Framework, given by $Aa^{3/2} - Fa^2$, together with the horizontal line corresponding to the synchronous condition = 1. The intersections define the two Clarke orbits a_{G1} and a_{G2}. The present orbit a_{now} lies to the left of a_{G1}, showing that TOI-5734 b is trapped in the collapsing death-spiral branch. Figure 9 illustrates the distinct tidal-evolution paths for sub synchronous and super synchronous regimes.

6.5 Collapsing death spiral

When a planet orbits inside the inner Clarke orbit, its orbital motion is faster than the stellar spin. In that regime, the tidal bulge raised on the star lags behind the planet in such a way that orbital angular momentum is extracted from the orbit and transferred to the stellar spin and internal dissipation. Consequently,

$$\dot{a} < 0. \tag{30}$$

Within the Primary-Centric Framework, this corresponds to a collapsing death spiral: the planet cannot tidally evolve outward toward the outer Clarke orbit, but instead undergoes secular orbital contraction. As the semi-major axis decreases, stellar irradiation, tidal forcing, and atmospheric escape all become stronger, reinforcing the coupled dynamical–thermal evolution discussed in the previous section.

Thus TOI-5734 b is not merely a planet near the radius valley; it is a transitional hot sub-Neptune that is already dynamically trapped in an inward orbital decay channel.

6.6 Physical implication for TOI-5734 b

The present system architecture indicates that TOI-5734 b is evolving through a combined sequence of

$$\textit{inward migration} \rightarrow \textit{enhanced irradiation} \rightarrow \textit{atmospheric erosion} \rightarrow \textit{continued inward tidal decay}$$

This makes the planet an important example of a close-in sub-Neptune whose structural transformation and orbital evolution are proceeding simultaneously. In this sense, the radius-valley position and the death-spiral dynamics are not independent properties but two manifestations of the same long-term evolutionary pathway.

6.7 Role of the Roche Limit in the Terminal Evolution

Figure 10 shows the progressive reduction in orbital separation due to tidal evolution. As tidal dissipation drives continued orbital decay, the planet moves progressively closer to its host star. In this regime, Roche geometry becomes increasingly important. The Roche limit defines the critical orbital distance at which tidal forces from the primary exceed the planet's self-gravity, leading to strong tidal distortion and potential mass loss [14,15].

Figure 11 presents a schematic overview of the system architecture and orbital configuration. For a fluid planet, the Roche limit is approximated by

$$a_{\text{Roche}} \approx 2.44\, R_p \left(\frac{M_\star}{M_p}\right)^{1/3}, \tag{31}$$

a relation derived for tidally distorted self-gravitating bodies [15]. Although TOI-5734 b presently remains outside this critical distance, sustained inward migration along the collapsing tidal branch will ultimately drive the planet into this regime.

As the outer atmosphere expands under strong stellar heating, it may approach the Roche-lobe boundary, significantly enhancing atmospheric escape [12].

Near the terminal stages of orbital evolution, tidal stripping and possible Roche-lobe overflow can rapidly remove the remaining volatile envelope [16,17]. Thus, while irradiation-driven escape likely dominates the current mass-loss phase, the Roche limit provides the boundary condition governing the final catastrophic stage of planetary evolution.

The long-term evolution of TOI-5734 b therefore follows a coupled sequence:

$$\textit{tidal decay} \rightarrow \textit{enhanced irradiation} \rightarrow \textit{atmospheric erosion} \rightarrow \textit{Roche-limit stripping}$$

6.8 Formation Beyond the Snow Line

Planets in the mass range of TOI-5734 b are commonly believed to form beyond the snow line of their natal protoplanetary disks, where volatile materials such as water ice are abundant. In these colder outer regions, solid material accumulates efficiently, enabling rapid core formation. Once a critical core mass is achieved, the planet can accrete a gaseous envelope from the surrounding nebula.

Given its present mass of 9.1 $M_\oplus$, TOI-5734 b likely originated as a volatile-rich proto-sub-Neptune, initially possessing a substantial hydrogen–helium atmosphere.

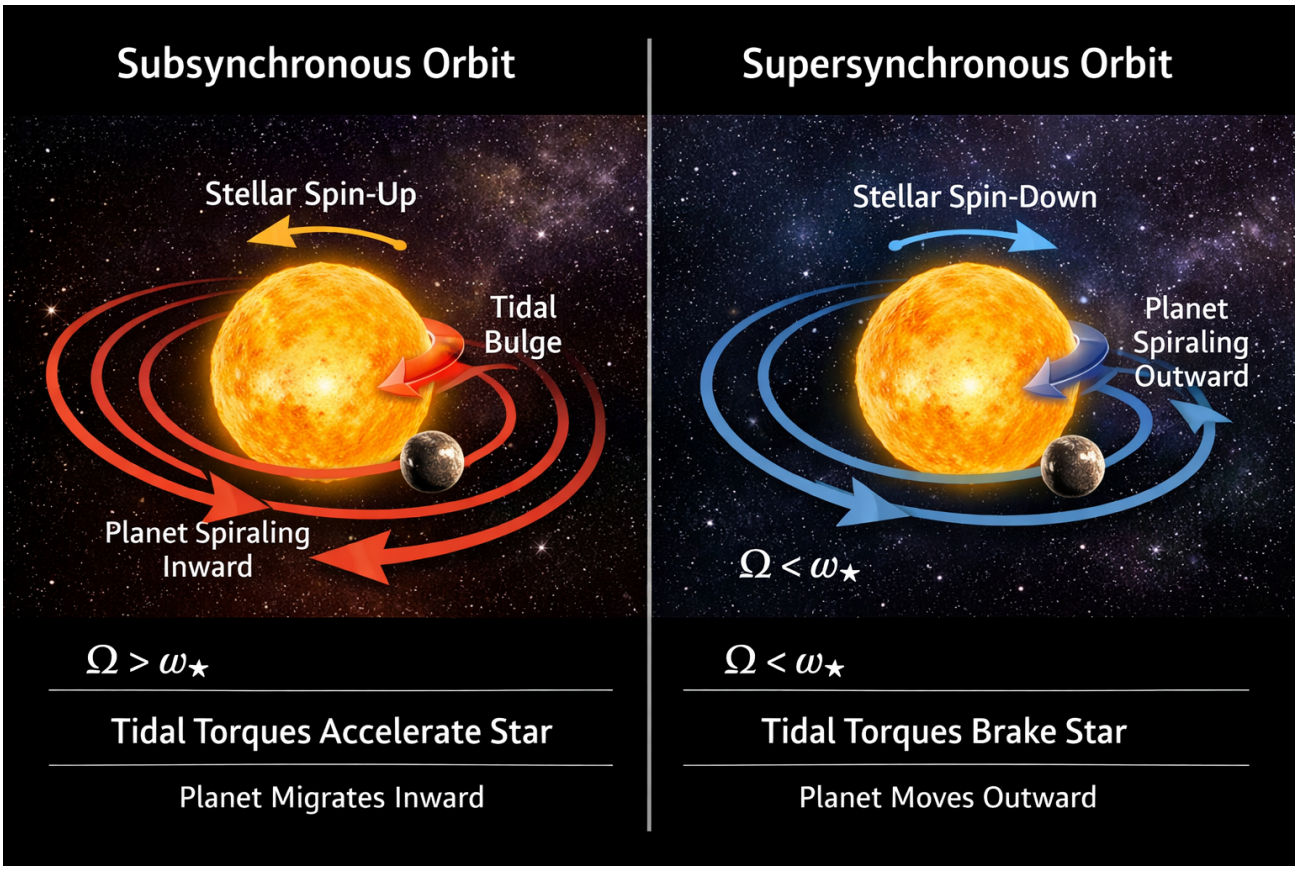

Figure 9: Tidal interaction regimes in star–planet systems. Left: Sub synchronous orbit ($\Omega > \omega_{\star}$). The orbital motion is faster than stellar rotation, causing the tidal bulge to lag behind the planet. Angular momentum is transferred from the orbit to the stellar spin and internal dissipation, leading to stellar spin-up and inward orbital migration of the planet (death-spiral evolution). Right: Super synchronous orbit ($\Omega < \omega_{\star}$). The star rotates faster than the orbital motion, and the tidal torque brakes the stellar spin. Angular momentum is transferred from stellar rotation to the orbit, causing the planet to migrate outward.

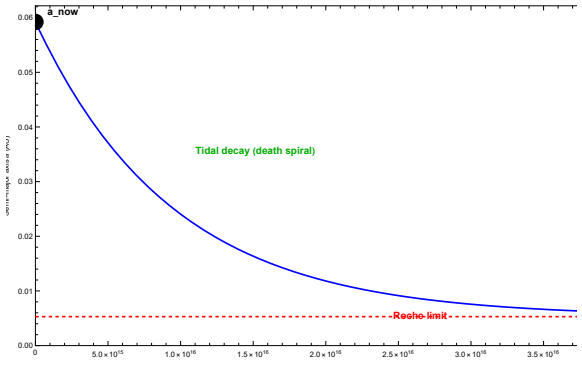

Figure 10: Illustrative tidal orbital decay of TOI-5734 b showing inward migration from the present orbit a_{now} toward the Roche-limit distance. The progressive reduction in orbital radius indicates long-term tidal dissipation leading to a collapsing death spiral.

6.9 Inward Orbital Migration

After formation, the planet likely migrated inward through interactions with the protoplanetary disk. Disk-driven Type I migration can efficiently transport intermediate-mass planets toward the inner regions of planetary systems on timescales shorter than disk lifetimes.

Additional inward evolution may have occurred through tidal interactions after disk dispersal. The present compact orbit($a \approx 0.06$ AU, $P = 6.18$ days) is consistent with substantial orbital migration from a formation site at larger orbital separations.

6.10 Onset of Intense Stellar Irradiation

As the planet approached its host star, stellar irradiation increased dramatically. Young K-dwarf stars emit enhanced X-ray and extreme-ultraviolet radiation, which strongly heats upper planetary atmospheres.

The resulting thermal expansion of the atmosphere reduces gravitational binding efficiency and initiates large-scale hydrodynamic escape.

6.11 Atmospheric Erosion Phase

Sustained atmospheric escape progressively removes the planet's primordial volatile envelope. Because planetary radius is highly sensitive to even small atmospheric mass fractions, envelope loss produces significant radius contraction. This process drives the planet toward the radius valley, marking the transition between gas-rich sub-Neptunes and rocky super-Earths. Evolutionary modeling indicates that TOI-5734 b may lose most of its primordial atmosphere within ~ 3 × 108 years, placing it in an advanced stage of atmospheric erosion.

[htbp]

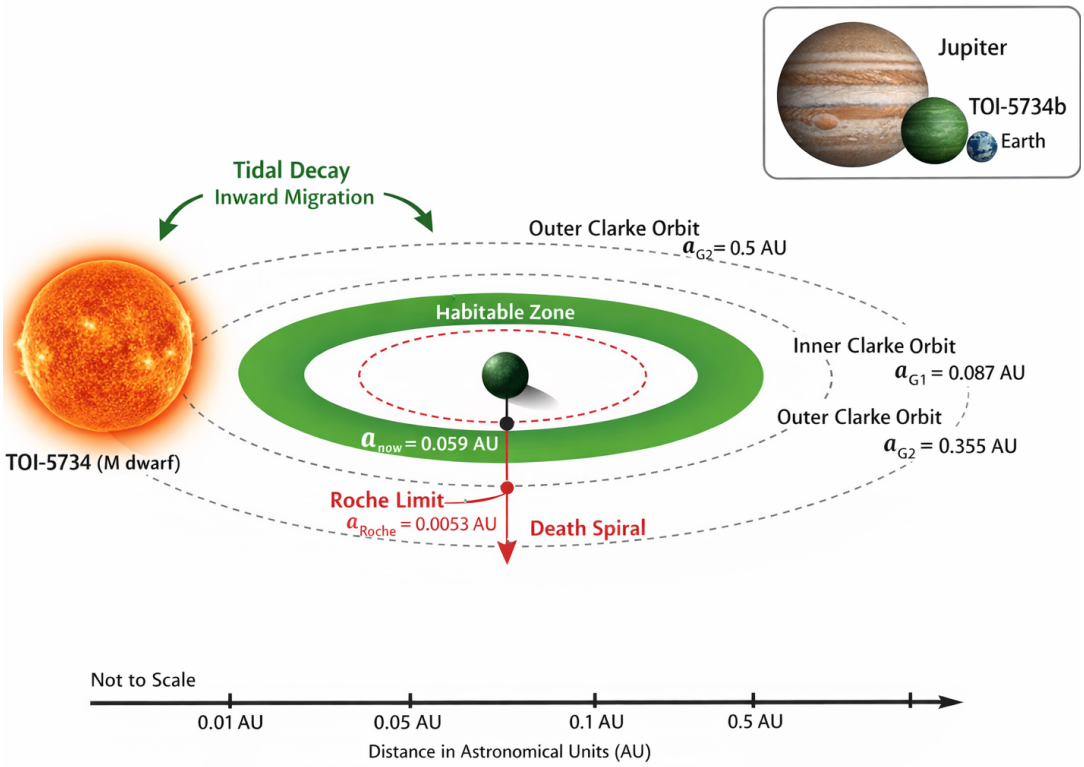

Figure 11. Schematic architecture of the TOI-5734 planetary system (not to scale). The present orbit of TOI-5734 b (a_{now} = 0.059 AU) lies interior to the inner Clarke orbit (a_{G1} = 0.087 AU), placing the planet on the inward tidal evolution branch. Continued tidal dissipation drives orbital decay toward the Roche-limit distance (a_{Roche} = 0.0053 AU), where tidal stripping and possible Roche-lobe overflow may occur. The outer Clarke orbit (a_{G2}) represents the stable synchronous boundary.[Credit: Original schematic created by the author with AI-assisted graphical rendering.]

6.12 Coupled Dynamical–Thermal Evolution

Orbital evolution and atmospheric escape are intrinsically linked. Tidal interactions gradually modify the semi-major axis and orbital energy, enhancing stellar irradiation and tidal heating. Within the Primary-Centric Framework, angular momentum exchange between orbital motion and stellar rotation regulates the long-term dynamical state of the system. Progressive inward migration amplifies atmospheric loss rates, while atmospheric mass reduction alters planetary structure and tidal response.

6.13 Transitional State Near the Radius Valley

The present physical parameters of TOI-5734 b— radius 2.1 $R_{\oplus}$, mass 9.1 $M_{\oplus}$, and short orbital period— place it near the upper boundary of the radius valley. This location strongly suggests that the planet is currently in a transitional evolutionary phase. TOI-5734 b therefore represents a snapshot of planetary transformation, bridging the evolutionary pathway between sub-Neptunes and super-Earths.

6.14 Long-Term Evolutionary Outcome

If atmospheric escape continues, the planet is expected to evolve toward a denser configuration resembling a rocky super-Earth with minimal volatile envelope. Its radius would decrease while mean density increases.

Such an evolutionary pathway provides a natural explanation for the observed bimodal radius distribution and supports the hypothesis that radius-valley planets are shaped by long-term atmospheric mass loss combined with orbital evolution.

7. Discussion

7.1 TOI-5734 b in the Context of Radius-Valley Planets

TOI-5734 b occupies a critical position near the upper boundary of the radius valley, placing it among a growing class of transitional planets that bridge the gap between rocky super-Earths and gas-rich sub-Neptunes. Such planets provide valuable empirical tests of competing theories that seek to explain the origin of the bimodal

radius distribution [3,4]. The planet's mass–radius combination suggests a predominantly rocky interior with a residual volatile envelope, consistent with partial atmospheric erosion. Its location in parameter space therefore supports evolutionary models in which atmospheric mass loss sculpts planetary demographics over time.

7.2 Comparison with Atmospheric Loss Mechanisms

Two principal mechanisms have been proposed to explain atmospheric erosion near the radius valley: photoevaporation driven by stellar high-energy radiation and core-powered mass loss driven by internal thermal luminosity.

The close orbital separation of TOI-5734 b implies intense stellar irradiation, favoring photoevaporation as a dominant driver of atmospheric escape. However, its intermediate mass and residual thermal content suggest that core-powered mass loss may also contribute. The system may therefore represent a regime where both mechanisms operate concurrently, providing a useful benchmark for theoretical models [5,6].

7.3 Dynamical Evolution and Tidal Interactions

The compact orbit of TOI-5734 b indicates strong tidal coupling between the planet and its host star. Tidal dissipation can modify orbital parameters over long timescales, potentially contributing to inward migration and orbital circularization [9]. Within the Primary-Centric Framework, angular momentum exchange between orbital motion and stellar rotation provides a quantitative measure of the system's dynamical state. Coupled orbital–thermal evolution may therefore accelerate atmospheric escape by increasing stellar irradiation and tidal heating as orbital distance decreases.

7.4 Implications for Planet Formation and Evolution

The evolutionary pathway inferred for TOI-5734 b supports a scenario in which intermediate-mass planets form with volatile envelopes beyond the snow line and subsequently migrate inward. Close-in irradiation then drives atmospheric stripping, transforming sub-Neptunes into denser super-Earths. This coupled migration–erosion pathway provides a natural explanation for the observed radius valley and suggests that present-day planetary demographics encode signatures of long-term evolutionary processes.

7.5 Observational Prospects

TOI-5734 b is a promising target for future observational campaigns. Transit spectroscopy with next-generation facilities could probe its atmospheric composition and constrain volatile mass fractions. High precision radial-velocity monitoring may refine mass estimates and reveal additional companions that influence dynamical evolution. Long-term timing observations could also detect tidal orbital decay, providing direct constraints on tidal dissipation efficiency and angular-momentum exchange processes.

7.6 Broader Significance

Transitional planets such as TOI-5734 b represent key laboratories for understanding how planetary systems evolve under the combined influence of formation history, irradiation environments, and dynamical interactions. Detailed characterization of such systems helps bridge the gap between theoretical models and observed exoplanet populations.

8. Conclusions

We have investigated the structural, atmospheric, and dynamical evolution of the recently discovered hot sub-Neptune TOI-5734 b, a short-period planet located near the upper boundary of the exoplanet radius valley. Our main results are summarized as follows:

(i) Transitional Planetary Regime: The mass (9.1 $M_{\oplus}$) and radius (2.1 $R_{\oplus}$) of TOI-5734 b place it in the transitional regime between rocky super-Earths and volatile-rich sub-Neptunes. Its bulk density suggests a predominantly rocky interior retaining a residual gaseous envelope.

(ii) Radius Valley Significance: The planet's position near the radius valley supports the interpretation that this feature marks an evolutionary boundary shaped by atmospheric mass loss. TOI-5734 b provides an observational probe of this transitional regime.

(iii) Atmospheric Escape: Strong stellar irradiation at a close orbital separation ($a \approx 0.06$ AU) favors hydrodynamic atmospheric escape. Evolutionary estimates indicate that the planet may lose most of its primordial volatile envelope within $\sim 3 \times 108$ years.

(iv) Interior Structure: Structural considerations are consistent with a multi-layered configuration consisting of a dense rocky core and a volatile envelope. Ongoing atmospheric erosion is expected to progressively increase mean density and reduce planetary radius.

(v) Orbital Evolution: The compact orbit implies significant tidal star–planet interactions. Within the Primary-Centric Framework, angular-momentum exchange between orbital motion and stellar rotation governs the long-term dynamical state and may enhance atmospheric escape through coupled evolution.

(vi) Evolutionary Pathway: A coherent evolutionary scenario emerges in which the planet formed beyond the snow line, migrated inward through disk and tidal interactions, and subsequently experienced irradiation driven atmospheric stripping. This migration– erosion pathway naturally explains its present transitional state.

(vii) Broader Implications: TOI-5734 b exemplifies the class of intermediate-mass planets whose present properties encode signatures of formation history, irradiation environment, and dynamical evolution. Such systems are essential for understanding the origin of the bimodal radius distribution in exoplanet populations. Future observational campaigns targeting atmospheric

composition, orbital evolution, and system architecture will further refine our understanding of transitional planets and the physical processes shaping planetary demographics [19-22].

Acknowledgments

I acknowledge Kesariya Food Court, Kalam Bagh Chawk, Muzaffarpur, Bihar, India, for financing the Article Processing Charge. This research is sponsored by UNIVERSITY GRANTS COMMISSION, India, under Emeritus Fellow scheme, EMERITUS/2012-13-GEN-855/. The Author acknowledges the help given by ChatGPT and deep seek in resolving difficult problems. Lastly, but not least, the Author acknowledges the services obtained from the computer system installed at the Maniari Radha Krishna Monastery in the Village and Post Mahanth Maniari Pin Code 843119., District Muzaffarpur, Bihar, in preparing this document.

Declaration Of Interests

The author declares no competing financial or non-financial interests.

Code Availability

The analysis code used in the study is available from the author on reasonable request.

References

1. Ricker, G. R., Winn, J. N., Vanderspek, R., Latham, D. W., Bakos, G. Á., Bean, J. L., ... & Villasenor, J. (2015). Transiting exoplanet survey satellite. Journal of Astronomical Telescopes, Instruments, and Systems, 1(1), 014003-014003.
2. Cosentino, R., Lovis, C., Pepe, F., Cameron, A. C., Latham, D. W., Molinari, E., ... & Weber, L. (2012, September). Harps-N: the new planet hunter at TNG. In Ground-based and airborne instrumentation for astronomy iv (Vol. 8446, pp. 657-676). SPIE
3. Fulton, B. J., Petigura, E. A., Howard, A. W., Isaacson, H., Marcy, G. W., Cargile, P. A., ... & Hirsch, L. A. (2017). The California-Kepler survey. III. A gap in the radius distribution of small planets. The Astronomical Journal, 154(3), 109.
4. Van Eylen, V., Agentoft, C., Lundkvist, M. S., Kjeldsen, H., Owen, J. E., Fulton, B. J., ... & Snellen, I. (2018). An asteroseismic view of the radius valley: stripped cores, not born rocky. Monthly Notices of the Royal Astronomical Society, 479(4), 4786-4795.
5. Owen, J. E., & Wu, Y. (2017). The evaporation valley in the Kepler planets. The Astrophysical Journal, 847(1), 29.
6. Ginzburg, S., Schlichting, H. E., & Sari, R. E. (2018). Core-powered mass-loss and the radius distribution of small exoplanets. Monthly Notices of the Royal Astronomical Society, 476(1), 759-765.
7. Lammer, H., Selsis, F., Ribas, I., Guinan, E. F., Bauer, S. J., & Weiss, W. W. (2003). Atmospheric loss of exoplanets resulting from stellar X-ray and extreme-ultraviolet heating. The Astrophysical Journal Letters, 598(2), L121-L124.
8. Lopez, E. D., & Fortney, J. J. (2013). The role of core mass in controlling evaporation: the Kepler radius distribution and the Kepler-36 density dichotomy. The Astrophysical Journal, 776(1), 2.
9. Jackson, B., Greenberg, R., & Barnes, R. (2008). Tidal evolution of close-in extrasolar planets. The Astrophysical Journal, 678(2), 1396-1406.
10. Filomeno, S., et al. 2026, Discovery and characterization of the hot sub- Neptune TOI-5734 b, arXiv e-prints, arXiv:2602.xxxxx
11. Watson, A. J., Donahue, T. M., & Walker, J. C. (1981). The dynamics of a rapidly escaping atmosphere: applications to the evolution of Earth and Venus. Icarus, 48(2), 150-166.
12. Erkaev, N. V., Kulikov, Y. N., Lammer, H., Selsis, F., Langmayr, D., Jaritz, G. F., & Biernat, H. K. (2007). Roche lobe effects on the atmospheric loss from "Hot Jupiters". Astronomy & Astrophysics, 472(1), 329-334.
13. Sharma, B. K. (2025). Hulse Taylor Pair Revisited in Primary-centric Frame-work. World Journal of Multidisciplinary Studies, 2(6), 1-15.
14. Roche, E. 1849, La figure d'une masse fluide soumise à l'attraction d'un point éloigné, Académie des Sciences de Montpellier, 1, 243–262
15. Chandrasekhar, S. (1987). Ellipsoidal figures of equilibrium. New York: Dover.
16. Gu, P.-G., Lin, D. N. C., & Bodenheimer, P. H. 2016, Roche-lobe overflow of short-period gaseous planets, The Astrophysical Journal, 588, 509–534
17. Jackson, B., Arras, P., & Penev, K. 2017, Tidal evolution of close-in exoplanets, The Astrophysical Journal, 835, 145
18. Darwin Darwin, G. H. 1879, On the precession of a viscous spheroid and on the remote history of the Earth, Philosophical Transactions of the Royal Society of London, 170, 447–530
19. Ferraz-Mello, S., Rodríguez, A., & Hussmann, H. (2008). Tidal friction in close-in satellites and exoplanets: The Darwin theory re-visited. Celestial Mechanics and Dynamical Astronomy, 101(1-2), 171-201.
20. Lanza, A. F. 2021, Tidal interactions in star–planet systems, Universe, 7, 185
21. Goldreich, P., & Soter, S. (1966). Q in the Solar System. icarus, 5(1-6), 375-389.
22. Owen, J. E., & Wu, Y. (2017). The evaporation valley in the Kepler planets. The Astrophysical Journal, 847(1), 29.